CHAPTER 4

EFFECTIVENESS FACTORS FOR PARTIALLY WETTED CATALYSTS

In this chapter, experimental wetting geometries are used to investigate reaction and diffusion in partially wetted catalysts. Models that describe these have been in existence for some time, and have been used with some success (Wu et al., 1996; Llano et al., 1997). The theorectical verification of existing models is usually based on easily definable theoretical wetting geometries such as spherical caps or rings (Goto et al., 1981; Yentekakis and Vayenas, 1987). All validations of existing and proposed models in this chapter are based on the realistic geometries obtained from the colorimetric experiments.

The estimation of catalyst effectiveness factors, defined as the ratio between the observed reaction rate in a pellet and the reaction rate in the absence of intraparticle mass transfer resistances, plays an important role in chemical reactor engineering and is governed by the solution to the reaction-diffusion equation within the catalyst:

$$\bigtriangledown^2 C - \phi^2 \times y(C) = 0 \tag{4.1}$$

where ϕ describes the ratio of reaction to diffusion and $y(C)$ is the kinetic expression in terms of the reagent concentration(s). The effectiveness factor can be evaluated by the integral of the reagent concentrations over the catalyst volume or the reagent fluxes over the catalyst's external area.

Exact analytical solutions for pellet efficiency factors are almost exclusively available for first- and zero-order reactions in pellets with well defined geometries[1] (Lee and Kim, 2006). Unique boundary conditions are also required, where the boundary condition at

[1]One-dimensional geometries for which analytical effectiveness factor derivations are available are those of an infinite slab, a sphere and an infinite cylinder.

the external surface is the same over the whole surface. Catalyst particles subject to trickle-flow generally do not confirm to these requirements:

- At least two reagents (a gas and a liquid) react in a trickle-bed reactor and the kinetic expression is probably not simply first order in one reagent. To simplify effectiveness factor derivations, the reaction in a trickle-bed reactor is usually classified as being either gas- or liquid-limited, i.e. the concentration of either the liquid or the gas reagent respectively is constant throughout the catalyst particle so that pseudo-first order kinetics can be assumed for the limiting reagent. A reaction is usually classified as gas- or liquid-limited based on γ, where

$$\gamma = \frac{\alpha D_B C_{B,bulk}}{D_A C_A^*} \tag{4.2}$$

  Throughout this chapter, B refers to the liquid and A to the gaseous reagent. A reaction is said to be gas-limited if $\gamma \gg 1$, and liquid-limited if $\gamma \ll 1$. Liquid-limited reactions are modelled differently from gas-limited reactions in trickle-beds.

- Boundary conditions for partially wetted particles are mixed, that is, the boundary condition for the wetted surface differs from that for the dry surface. Except for specific (theoretical) wetting and particle geometries, mixed boundary conditions will increase the dimensionality of Equation (4.1).

The chapter deals with the following questions surrounding pellet efficiency in trickle-bed reactors:

- What is the performance of existing models for liquid-limited and gas-limited reactions? Investigations that deal with this question already exist (Goto et al., 1981; Mills and Dudukovic, 1979) but not where true partial wetting geometries are used. In this chapter, the true wetting geometries shown in Figure 3.10 are used in the investigation.

- When can a reaction be classified as liquid- or gas limited, and is it possible to reconcile models for gas- and liquid-limited reactions in the case where both reagents play a role? For this purpose, the reaction $r_A = \alpha r_B = -\alpha k_r C_A C_B$ taking place in a partially wetted catalyst is investigated. A numerical study of this reaction was also performed by Yentekakis and Vayenas (1987), but no suggestions were made for an easy-to-use analytical expression.

- Many trickle-bed reactors make use of eggshell catalysts. Though it is rather easy to derive analytical expressions for a completely wetted eggshell catalyst with first-order reaction kinetics, the role of partial wetting may differ significantly for eggshell catalysts than for monodispersed catalysts. The effect of partial wetting on the performance of this type of catalyst is therefore also investigated.

The work is based on the numerical modelling of partially wetted monodispersed and eggshell catalyst spheres, using the finite element method (FEM) and true wetting geometries obtained from the work discussed in Chapter 3. FEM is used since it can easily handle complex geometries and is also suitable for higher order kinetic expressions (Mills et al., 1988; Ramachandran, 1991). All work is limited to isothermal conditions.

4.1 Numerical method

4.1.1 First-order reaction, $-r = k_r C$

Models for gas- and liquid-limited reactions in partially wetted catalysts assume a constant concentration of the non-limiting reagent and first-order kinetics for the limiting reagent so that the reaction can be written as $-r = k_r C$. In dimensionless form, the equation for steady-state diffusion combined with such a reaction within a catalyst sphere is given by

$$\nabla^2 c - \phi^2 c = 0 \tag{4.3}$$
$$c = \frac{C}{C_{bulk}};\ \phi = r_p \sqrt{\frac{k_r}{D}}$$

Hence, one wants to solve the following integral:

$$\int_V \left[\nabla^2 c - \phi^2 c\right] \cdot w \ dV = 0 \tag{4.4}$$

where w is any one of all possible weighting functions, and V is the body for which the diffusion-reaction equation will be solved. Making use of the product rule, Equation 4.4 can be written as:

$$\left[\int_V \nabla \cdot (w \nabla c) \ dV - \int_V \nabla w \nabla c \ dV\right] - \int_V \phi^2 c \cdot w \ dV = 0 \tag{4.5}$$

The boundary conditions can be accounted for by making use of the Gauss divergence theorem (analogous to a mass balance over the body):

$$\int_V \nabla \cdot f \ dV = \int_S f \cdot \overline{n} \ dA \tag{4.6}$$
$$\therefore \int_V \nabla (w \nabla c) \ dV = \int_S w \nabla c \cdot \overline{n} \ dA \tag{4.7}$$
$$\text{and } \nabla c \cdot \overline{n} = Bi\,(1 - c)\,; \text{ where } Bi = \frac{k_c r_p}{D} \tag{4.8}$$

And Equation (4.5) can be written as:

$$\int_S Bi(1-c)\cdot w\ dA - \int_V \bigtriangledown c \bigtriangledown w\ dV - \int_V \phi^2 c\cdot w\ dV = 0 \tag{4.9}$$

Equation (4.9) is valid for any body V with external area S. In the finite element method, V is divided into small elements v with concentrations $\{c\}$ at each node point. The concentration at any point within the volume is approximated by an interpolation matrix, $[N]$.

$$\begin{aligned} c(x,y,z) &= [N]\{c\} \\ w(x,y,z) &= [N]\{w\} \\ &\text{and} \\ \bigtriangledown c(x,y,z) &= [B]\{c\} \\ \bigtriangledown w(x,y,z) &= [B]\{c\} \end{aligned} \tag{4.10}$$

where $[B] = \bigtriangledown[N]$ and $\{w\}$ is the value of w at each node point. Note that $[N]$ and $[B]$ are functions of the element geometry only, and that $\{c\}$ is only defined for the node points. $[N]$ and $[B]$ are specific to each element and differ for the surface integral from that for the volume integrals. More information on the choice of element geometry and the contruction of $[N]$ and $[B]$ can be found in any textbook on finite element methods, for example Cook et al. (1989). For each element

$$\begin{aligned} &\int_s Bi(1-c)\cdot w\ dA - \int_v \bigtriangledown c \bigtriangledown w\ dV - \int_v \phi^2 c\cdot w\ dV \\ &\approx \{w\}^T \left[\int_s [N]^T Bi\ dA - \{c\}\int_s [N]^T[N] Bi\ dA \right. \\ &\left. -\{c\}\int_v [B]^T[B]\ dV - \{c\}\int_v \phi^2 [N]^T[N]\ dV\right] \end{aligned} \tag{4.11}$$

Equation (4.9) can be approximated by the sum of above integrals for all elements v in the volume V:

$$\begin{aligned} &\sum_v^V \{w\}^T \left[\int_s Bi[N]^T\ dA - \{c\}\int_s Bi[N]^T[N]\ dA \right. \\ &\left. -\{c\}\int_v [B]^T[B]\ dV - \{c\}\int_v \phi^2 [N]^T[N]\ dV\right] = 0 \end{aligned} \tag{4.12}$$

The integrals for each specfic element are obtained according to a specified concentration variation within each element as a function of the nodal concentrations (e.g. linear or quadratic variation). Since Equation (4.12) should hold true for all possible weighting

functions w:

$$\sum_{v}^{V}\left[\left(\int_{v}[B]^{T}[B]\ dV\ +\ \int_{v}\phi^{2}[N]^{T}[N]\ dV+\int_{s}Bi[N]^{T}[N]\ dA\right)\{c\}\right]$$
$$=\sum_{v}^{V}Bi\int_{s}[N]^{T}\ dA \tag{4.13}$$

Which is of the form

$$\underbrace{[K]}_{n\times n}\times\underbrace{\{c\}}_{n\times 1}=\underbrace{[F]}_{n\times 1}$$

The stiffness matrix $[K]$ and vector $[F]$ are functions of the geometry and known constants only, so that the nodal concentrations $\{c\}$ can be solved for, solving a system of linear equations.

4.1.2 Reactions of the form $r_A = \alpha r_B = -\alpha k_r C_A C_B$

In dimensionless form, the reaction-diffusion equations for the reaction $r_A = \alpha r_B = -\alpha k_r C_A C_B$ in a spherical pellet are:

$$\begin{aligned}\bigtriangledown^2 a &- \phi_A^2 ab = 0\\ \bigtriangledown^2 b &- \phi_B^2 ab = 0\\ a &= \frac{C_A}{C_{A,\ bulk}};\ \phi_A = r_p\sqrt{\frac{\alpha k_r C_{B,\ bulk}}{D_A}}\\ b &= \frac{C_B}{C_{B,\ bulk}};\ \phi_B = r_p\sqrt{\frac{k_r C_{A,\ bulk}}{D_B}}\end{aligned} \tag{4.14}$$

Following the same route as Equations (4.4) to (4.13), the FEM equations for this reaction are:

$$\left[\sum_{V}\left(\int_{v}[B]^{T}[B]\ dV+\int_{s}Bi_A[N]^{T}[N]\ dA\right.\right.$$
$$\left.\left.+\ \int_{v}\phi_A^2[N]^{T}[N]\{b\}[N]\ dV\right)\right]\cdot\{a\}=\sum_{S}\int_{s}Bi_A[N]^{T}\ dA \tag{4.15}$$

$$\left[\sum_{V}\left(\int_{v}[B]^{T}[B]\ dV+\int_{s}Bi_B[N]^{T}[N]\ dA\right.\right.$$
$$\left.\left.+\ \int_{v}\phi_A^2[N]^{T}[N]\{a\}[N]\ dV\right)\right]\cdot\{b\}=\sum_{S}\int_{s}Bi_B[N]^{T}\ dA \tag{4.16}$$

$$\tag{4.17}$$

Since both equations contain the terms $\{a\}$ and $\{b\}$, the equations cannot be solved in the same fashion as Equation (4.13). The coupled system can be solved by defining the residuals R_A and R_B that should be equal to 0 for the correct concentration profiles:

$$\begin{aligned} R_A &= \left[\sum_V \left(\int_v [B]^T[B]\ dV + \int_s Bi_A[N]^T[N]\ dA \right.\right. \\ &+ \left.\left. \int_v \phi_A^2[N]^T[N]\{b\}[N]\ dV\right)\right] \cdot \{a\} - \sum_S \int_s Bi_A[N]^T\ dA \end{aligned} \tag{4.18}$$

$$\begin{aligned} R_B &= \left[\sum_V \left(\int_v [B]^T[B]\ dV + \int_s Bi_B[N]^T[N]\ dA \right.\right. \\ &+ \left.\left. \int_v \phi_A^2[N]^T[N]\{a\}[N]\ dV\right)\right] \cdot \{b\} - \sum_S \int_s Bi_B[N]^T\ dA \end{aligned} \tag{4.19}$$

The concentration profiles for which R_A and R_B are approximately zero were found by using the Newton-Rhapson iterative scheme for coupled non-linear systems:

$$\begin{bmatrix} \frac{\partial R_A}{\partial\{a\}} & \frac{\partial R_A}{\partial\{b\}} \\ \frac{\partial R_B}{\partial\{a\}} & \frac{\partial R_B}{\partial\{b\}} \end{bmatrix} \times \begin{Bmatrix} \Delta a \\ \Delta b \end{Bmatrix} = - \begin{Bmatrix} R_A \\ R_B \end{Bmatrix} \tag{4.20}$$

$$\left.\begin{Bmatrix} a \\ b \end{Bmatrix}\right|_{i+1} = \left.\begin{Bmatrix} a \\ b \end{Bmatrix}\right|_i + \left.\begin{Bmatrix} \Delta a \\ \Delta b \end{Bmatrix}\right|_i \tag{4.21}$$

This solution strategy requires the inversion of matrices of double the size of that for a first-order reaction when the same FEM grid is used, and is therefore more computationally intensive.

4.1.3 Meshing

A tetrahedral mesher for Matlab that was developed by Persson and Strang (2004) was used to generate 3-dimensional meshes of a sphere. In total, six different meshes were used for the investigation: Simulations of monodispersed and eggshell particles were performed with different meshes, since the shell had to be well-defined for the simulation of eggshells. For a grid size of n nodes, the solution of Equation (4.13) requires the solution of an $n \times n$ system, whereas the iterative solution of Equations (4.18) to (4.20) requires the (iterative) solution of a $2n \times 2n$. Therefore, computational limitations required the meshes for the reaction $-r_A = \alpha k_r C_A C_B$ to be coarser than the corresponding meshes for first-order reactions. Meshes were created for both reactions, monodispersed particles; and eggshell particles with inner to outer shell diameter rations of $\rho = 0.9$ and $\rho = 0.5$. Cross-sections of the meshes for the monodispersed particles an eggshell particles with $\rho = 0.9$ are shown in Figure 4.1.

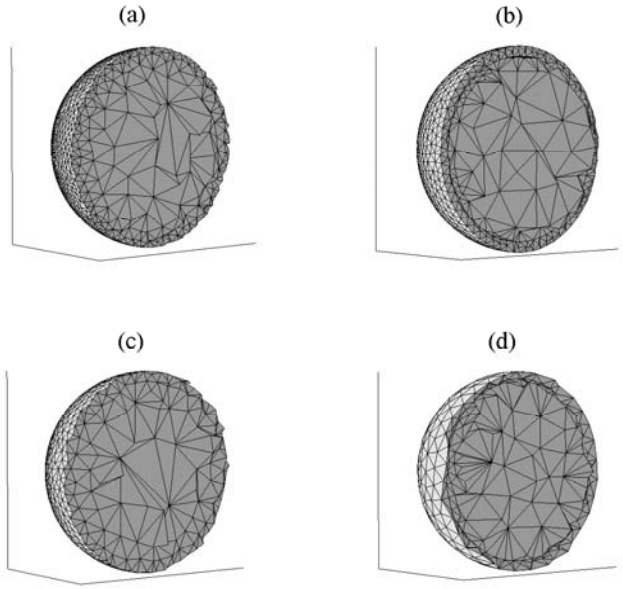

Figure 4.1: Finite element meshes for (a) a first order reaction in a monodispersed particle; (b) a first order reaction in an eggshell particle; (c) a reaction of the form $-r_A = k_r C_A C_B$ in a monodispersed particle; (d) a reaction of the form $-r_A = k_r C_A C_B$ in an eggshell particle.

Boundary conditions are based on the wetting geometries shown in Chapter 3, Figure 3.10: each surface triangle in the grid is assigned a Biot number based on its wetting condition (wet or dry). For the liquid reagent, $Bi_{B,d} = 0$ and for the gas reagent $Bi_{A,d} \gg Bi_{A,w}$. Note that the resolution at which the wetting geometry could be specified is a function of the mesh resolution. Quadratic interpolation matrices were used for the integration of the mesh elements. These were found to be more suited to the typical concentration profiles than linear interpolation.

4.1.4 FEM accuracy

The FEM solution for a first-order elementary reaction can be verified with the following analytical expressions for the concentration profile in the absence of external mass transfer

resistances:

For monodispersed catalyst:

$$c(\lambda) = \frac{\sinh(\phi \cdot \lambda)}{\sinh \phi} \tag{4.22}$$

For an eggshell catalyst:

$$c(\lambda) = \frac{A_1 e^{\phi \cdot \lambda} + A_2 e^{-\phi \cdot \lambda}}{\lambda} \qquad \rho \leq \lambda \leq 1 \tag{4.23}$$

$$c(\lambda) = c(\rho) \qquad \lambda \leq \rho$$

$$A_1 = \left(e^{\phi} + e^{\phi(1-2\rho)} \frac{\phi - \frac{1}{\rho}}{\phi + \frac{1}{\rho}} \right)^{-1}$$

$$A_2 = e^{\phi} - A_1 e^{2\phi}$$

Here, $c(\lambda)$ is the dimensionless radial concentration profile, and $\rho = r_s/r_p$ where r_s is the inner dimension of the catalyst shell. Solutions are accurate and numerically stable for $\phi \leq 30$, as is shown in Figure 4.2.

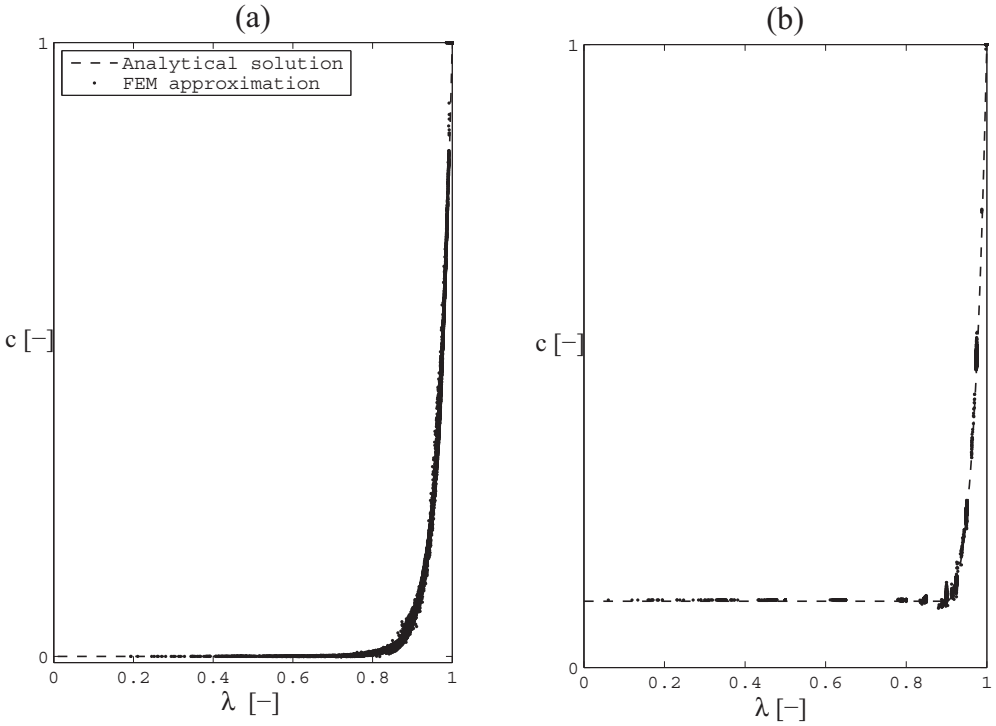

Figure 4.2: Numerical solutions for (a) a monodispersed catalyst and (b) an eggshell catalyst for $\phi = 30$ and no external mass transfer tested against the analytical solutions given in Equations (4.22).

For the reaction $-r_A = -\alpha r_B = \alpha k_r C_a C_b$ the FEM solutions can be verified as follows.

- For symmetric boundary conditions, $\phi_A \gg \phi_B$ and no external mass transfer resis-

tances, the concentration profile of reagent A should be given by Equations (4.22).

- For symmetric boundary conditions and any value of ϕ'_A and ϕ'_B, the following relationship should hold true[2]:

$$b = \frac{a - 1 + \gamma'}{\gamma'} \qquad (4.24)$$
$$\gamma' = \left(\frac{\phi'_A}{\phi'_B}\right)^2$$

  Unlike ϕ_A and ϕ_B, which are based on bulk concentrations, ϕ'_A and ϕ'_B are based on reagent surface concentrations. The same applies to γ'.

The derivation for this relationship is shown in Appendix A. Numerical and analytical concentration profiles are shown in Figure 4.3. Since the concentration profile is sharper for a higher Thiele modulus, increasingly smaller elements are required near the surface as the Thiele modulus increases. The meshes that were used are limited to a maximum Thiele modulus of 30, beyond which inaccuracies became unacceptably large. Note that the steepest concentration profiles are those shown in the figure, and not where $\phi_A = \phi_B = 30$ as one may intuitively expect.

4.2 Monodispersed particles

Preliminary results of the FEM simulations showed that the behaviour of partially wetted monodispersed catalysts differs significantly from that of eggshell catalysts. In this section, the behaviour of partially wetted monodispersed catalysts and different reaction expressions is described, based on FEM results.

4.2.1 Theory

To obtain an understanding of the behaviour of partially wetted monodispersed catalysts for different reaction cases, it is first neccesary to understand the relevant existing theories.

Geometry

For the theoretical particle geometries of a semi-infinite slab, a semi-infinite cylinder[3] and a sphere, a first-order reaction and a single boundary condition at the external surface,

[2]Note that for a reaction that is first order in A and in B, $\left(\frac{\phi_A}{\phi_B}\right)^2 = \frac{\alpha D_B C_{B,bulk}}{D_A C_A^*}$

[3]A semi-infinite slab has a finite thickness L and an infinite height, and a semi-infinite cylinder has a finite radius r_C and an infinite height.

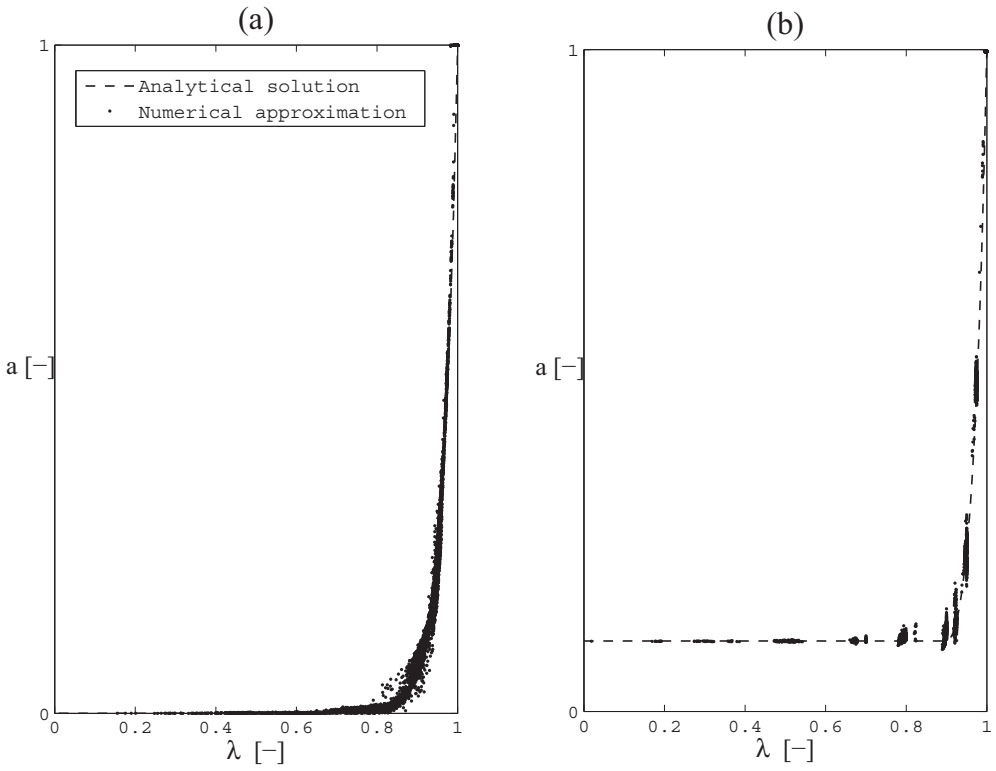

Figure 4.3: Numerical and analytical solutions for the reaction $r_A = \alpha r_B = -\alpha k_r C_A C_B$ for the case where $\phi_A \gg \phi_B = 30$. (a) Monodispersed particle, (b) eggshell particle with $\rho = 0.9$.

Equation (4.1) is one-dimensional; and exact analytical expressions for the pellet efficiency can derived:

$$\text{Semi-infinite slab: } \eta = \frac{\tanh \phi_G}{\phi_G} \quad \left(\phi_G = L\sqrt{\frac{k_r}{D}} = \frac{V_R}{S_x}\sqrt{\frac{k_r}{D}}\right) \tag{4.25}$$

$$\text{Semi-infinite cylinder: } \eta = \frac{2I_1(\phi_C)}{\phi_C I_0(\phi_C)} \quad \left(\phi_C = r_C\sqrt{\frac{k_r}{D}} = \frac{2V_p}{S_x}\sqrt{\frac{k_r}{D}}\right) \tag{4.26}$$

$$\text{Sphere: } \eta = \frac{3}{\phi^2}\left(\phi \coth \phi - 1\right) \quad \left(\phi = r_p\sqrt{\frac{k_r}{D}} = \frac{3V_p}{S_x}\sqrt{\frac{k_r}{D}}\right) \tag{4.27}$$

Aris (1957) showed that the efficiencies of all the above geometries have more or less the same functionality with the modulus of a slab, $\phi_G = L(k_r/D)^{1/2}$ (termed the generalised modulus), where L is the ratio between the particle volume and external area. He therefore proposed to use Equation (4.25) to approximate pellet efficiency factors, regardless of the particle shape. The maximum error encountered when modelling a sphere as a slab, is approximately 10% at intermediate ϕ. In the limits of $L \to 0$ and $L \to \infty$, efficiency factors for spheres, cylinders and slabs are exactly the same for the same ϕ_G. The idea of a generalised modulus form the basis for modeling partially wetted particles under liquid-limited reaction conditions.

One-dimensional geometries are not necessarily limiting cases in terms of the modulus-efficiency relationship and there is no guarantee that this relationship will be close to that of a slab for all geometries. Burghardt and Kubaczka (1996) therefore suggested a different approach where not only the modulus, but also the modulus-efficiency relationship is determined by the shape of the particle. This work is based on the fact that the efficiency expressions for the three 1-D geometries can be written in terms of modified Bessel functions of the first kind[4]:

$$\eta = \frac{h+1}{\phi''}\frac{I_{(h+1)/2}(\phi'')}{I_{(h-1)/2}(\phi'')} \tag{4.28}$$

where $h = 0, 1$ and 2, for a slab, a cylinder and a sphere respectively. The modulus ϕ'' is the modulus relevant to each geometry. Therefore, these authors propose the following expression which not only generalises the modulus but also the modulus-efficiency

[4]Modified Bessel functions are general solutions to the differential equation of diffusion and reaction in a semi-infinite cylinder. As for any second-order differential equation, two general solutions exist - in this case the modified Bessel functions of the first and second kind, $I_0(x)$ and $K_0(x)$

relationship for a given geometry:

$$\eta = \frac{h+1}{\phi_{GC}} \frac{I_{(h+1)/2}(\phi_{GC})}{I_{(h-1)/2}(\phi_{GC})}$$
$$h = \frac{S_p.R'}{V_p} - 1$$
$$\phi_{GC} = R' \sqrt{\frac{k_r}{D}} \tag{4.29}$$

where R' is the maximum reagent penetration depth along the most favourable diffusion path. More information on how to calculate R' for a given geometry can be found in the paper by these authors (Burghardt and Kubaczka, 1996). This method is commonly known as the generalised cylinder (GC) method. The GC model has never been used before in the modelling of partially wetted particles.

The expressions so far are for pellet efficiency factors and do not take external mass transfer resistances into account. To obtain an overall efficiency factor which takes external mass transfer resistances into account, one can make use of the following relationship:

$$\eta_0 = \eta \frac{C_s}{C_{bulk}} = \eta \left(1 + \frac{(\phi_G)^2 \eta}{Bi''} \right)^{-1} \tag{4.30}$$
$$Bi'' = \frac{V_R k_c}{S_x D} \tag{4.31}$$

This relationship can be derived from the equality:

$$S_x k_c \left(C_{bulk} - C_s \right) = V_R \eta k_r C_s \tag{4.32}$$

Modelling of partial wetting

Effectiveness factors for particles in trickle-bed reactors are complicated by the fact that the boundary conditions for Equation (4.1) are mixed: Due to incomplete wetting, two boundary conditions must be satisfied, one for the wetted and one for the dry surface. Even for the 1-D geometries of a sphere, a slab and a cylinder, the diffusion-reaction problem obtains extra dimensions[5].

For liquid-limited reactions, Dudukovic (1977) made use of the work of Aris (1957) to derive an expression for the catalyst efficiency of partially wetted particles for liquid-limited reactions, realising that only the wetted area can supply the reagent so that $S_x = S_p \cdot f$:

$$\eta = \frac{\tanh \phi_G}{\phi_G} \quad \text{where: } \phi_G = \frac{V_p}{f \cdot S_p} \sqrt{\frac{k_r}{D}} \tag{4.33}$$

The above equation suggests that partial wetting affects the effective geometry of a par-

[5]Exceptions are the geometries defined by Beaudry et al. (1987) and Valerius et al. (1996a)

ticle due to its effect on the external area available for reagent supply. It is important for the rest of this chapter to realise that if all shapes can be approximated for a slab with $L = V_R/S_x$ then it should also be possible to approximate all shapes with a sphere, so that Equation (4.33) becomes:

$$\eta = \frac{3f^2}{\phi^2}\left(\frac{\phi}{f}\coth\left(\frac{\phi}{f}\right) - 1\right) \quad \text{where: } \phi = \frac{3V_p}{S_p}\sqrt{\frac{k_r}{D}} \tag{4.34}$$

The overall efficiency that takes external mass transfer limitations into account can easily be modelled, making use of Equation (4.30), and taking into account that only the wetted area is available for external mass transfer:

$$\begin{aligned} \eta_0 &= \eta\frac{C_s}{C_{bulk}} = \eta\left(1 + \frac{(\phi_G)^2\eta}{Bi''}\right)^{-1} \\ &= \frac{\tanh\phi_G}{\phi_G\left(1 + \frac{\phi_G\tanh\phi_G}{Bi'_w f}\right)} \quad \text{Slab geometry} \end{aligned} \tag{4.35}$$

$$\text{or} \qquad \frac{3f^2\left(\frac{\phi}{f}\coth\frac{\phi}{f} - 1\right)}{\phi^2\left(1 + \frac{f\left(\frac{\phi}{f}\coth\frac{\phi}{f} - 1\right)}{Bi_w}\right)} \quad \text{Sphere geometry} \tag{4.36}$$

The above approach can not be followed for a gas-limited reaction, since the gas enters via both the wetted and the dry surface area. The most widely accepted model for a gas-limited reaction in a partially wetted catalyst was provided by Ramachandran and Smith (1979). The model is based on infinite slab geometry and the assumption that the reactant entering through the dry part and the wetted part of the slab can be treated separately and do not interact throughout the slab volume:

$$\eta_0 = \frac{f\cdot\tanh\phi_G}{\phi_G\left(1 + \frac{\phi_G\tanh\phi_G}{Bi'_w}\right)} + \frac{(1-f)\cdot\tanh\phi_G}{\phi_G\left(1 + \frac{\phi_G\tanh\phi_G}{Bi'_d}\right)} \tag{4.37}$$

When compared to Equation (4.30), it is clear that this expression is analagous to that of a slab where the entire surface is at a surface concentration $\overline{C_s}$, where $\overline{C_s} = f \times C_{s,w} + (1-f)\times C_{s,d}$. When using Equation (4.37), it is important to realise that this equation views gas-liquid-particle surface mass tranfer as one step, so that Bi_w is a combined Biot number for gas-liquid and liquid-solid mass transfer. This can be done when the rate of liquid-solid and gas-liquid mass transfer is the same. For high conversions of the liquid reagent and negligible expense of the gas, this is a reasonable assumption. When the inlet condition (e.g. saturated liquid, or zero gas-side reagent in the liquid) is of importance[6], the differential description of the concentration profile of the gaseous reagent in the liquid

[6]For example at low conversions

that is necessary to evaluate the overall reaction rate r, analogous to equation (4.37), is:

$$\begin{aligned}\frac{dC_{bulk}}{dV_c} = k_{GL}a_{GL}\left(C* - C_{bulk}\right) - k_{LS}a_p f\left(C_{bulk} - C_{s,w}\right) \\ k_{LS}a_p\left(C_{bulk} - C_{s,w}\right) = \eta k_R C_{s,w} \\ -r = f\eta k_R C_{s,w} + \left(1-f\right)\eta k_R C^* \end{aligned} \tag{4.38}$$

Clearly, the modelling of gas-limited reactions is completely different from that of liquid-limited reactions: the limit of equation (4.37) where $Bi_d \rightarrow 0$ is only the same as the liquid-limited description of equation (4.35) at large moduli.

Valerius et al. (1996b) suggested a particle efficiency model which can take wetting efficiency into account and can be used for gas-limited *and* liquid-limited reactions. The model is based on a hollow cylinder geometry where the outer surface area represents the wetted area and the inner surface the dry area of a partially wetted pellet, and can therefore only be used for $f > 0.5$. This geometry is used in a later paper (Valerius et al., 1996a) to simplify the numerical calculations for intricate kinetic expressions by transforming a 3-D problem to a 2-D problem, rather than to obtain analytical expressions for pellet efficiency factors. Only the analytical expression for a liquid-limited reaction was reported and will be verified in this chapter.

Kinetics

Exact explicit expressions of pellet efficiency factors only exist for simple kinetic expressions such as zero and first order kinetics (Lee and Kim, 2006). Large amounts of literature are therefore available, which present methods of approximating effectiveness factors for arbitrary kinetics. Probably the most important amongst these is that of Bischoff (1965), who suggested a general modulus for kinetics of any form. This modulus has more or less the same effect on pellet efficiency independent of the kinetic expression. To understand how the Bischoff modulus can be used, a short version of the derivation

of this modulus is now shown:

The diffusion-reaction equation in a slab is given by:

$$D\frac{d^2C}{dx^2} = r(C) \quad \left(C(0) = C_s; \quad \left.\frac{dC}{dx}\right|_{x=L} = 0\right) \tag{4.39}$$

$$\text{Let: } p = \frac{dC}{dx}, \text{ then: } \frac{d}{dx} = p \cdot \frac{d}{dC}$$

$$\therefore r(C) = D\frac{d^2C}{dx^2} = D \cdot p\frac{dp}{dC} = \frac{D}{2}\frac{d}{dC}\left(p^2\right) \tag{4.40}$$

Integrate from $p = 0$ (at $x = L$) to p:

$$\int_0^p d\left(p^2\right) = \frac{2}{D}\int_{C_L}^{C} r(\beta)d\beta$$

$$\therefore p^2 = \frac{2}{D}\int_{C_L}^{C} r(\beta)d\beta$$

$$\text{and} \quad \frac{dC}{dx} = p = -\sqrt{\frac{2}{D}}\left(\int_{C_L}^{C} r(\beta)d\beta\right)^{1/2} \tag{4.41}$$

The effectiveness factor can be evaluated using the flux of reagent into the slab:

$$\begin{aligned}\eta &= \frac{-S_pD \cdot \left.\frac{dC}{dx}\right|_{x=0}}{V_pr(C_s)} \\ &= \frac{S_p\sqrt{2D}\left(\int_{C_L}^{C_s} r(\beta)d\beta\right)^{1/2}}{V_pr(C_s)}\end{aligned} \tag{4.42}$$

It is well known that for simple order reactions in a slab, the pellet efficiency factor - Thiele modulus curve has the relationship $\eta = \phi_G^{-1}$ when $\phi_G \gg 1$. At such high Thiele moduli, L or r is very large and $C_L \to C_{eq}$, where C_{eq} is the concentration where $r(C_{eq}) \to 0$. For example $C_{eq} = 0$ when a reaction is irreversible and involves only one reagent. To have the same behaviour for an arbitrary reaction at a large Bischoff modulus (large L and/or fast reaction), this modulus can be defined as:

$$\phi_T'' = \left(\eta_{C_{eq}}\right)^{-1} = \frac{V_p \cdot r(C_s)}{S_p\sqrt{2D}}\left(\int_{C_{eq}}^{C_s} r(\beta)d\beta\right)^{-1/2} \tag{4.43}$$

In the original work, the diffusivity was also allowed to vary as a function of concentration, resulting in the following expression for the Bischoff modulus:

$$\phi_T'' = \frac{V_p \cdot r(C_s)}{S_p\sqrt{2}} \left(\int_{C_L}^{C_s} D(\beta) r(\beta) d\beta \right)^{-1/2} \tag{4.44}$$

Where the derivation of Bischoff (1965) was done for a slab (to be used with Equation 4.25), one can for the same reasons as discussed earlier, define a "spherical" Bischoff modulus that can be used with Equation (4.27):

$$\phi_T = \frac{3V_p \cdot r(C_s)}{S_p\sqrt{2D}} \left(\int_{C_{eq}}^{C_s} r(\beta) d\beta \right)^{-1/2} \tag{4.45}$$

4.2.2 Verification of existing models

Efficiency factors for partially wetted catalysts are only available for completely liquid-limited and completely gas-limited reactions where only one of the reagents plays a role. The accuracy of these models can now be evaluated with the FEM models for true wetting geometries. In this section, the Bischoff approximation for the reaction $-r_A = \alpha k_r C_A C_B$ is also derived and verified for fully wetted particles.

Liquid-limited reactions

Monodispersed particle efficiencies of all the photographed particles shown in Figure 3.10 were calculated for $0.1 \leq \phi \leq 30$ in the absence of external mass transfer resistances. Results are shown in Figure 4.4 as a function of the generalised modulus for partially wetted particles as suggested by Dudukovic (1977). It is clear from the figure that this approach yields rather good results, as can also be inspected by the parity plot in the top left corner.

It is proposed that, as for the generalised modulus approach, the GC method can be adapted to model the effect of partial wetting on liquid-limited reactions wetting by adjusting the "effective geometry":

$$\begin{aligned} \eta &= \frac{h+1}{\phi_{GC}} \frac{I_{(h+1)/2}(\phi_{GC})}{I_{(h-1)/2}(\phi_{GC})} \\ \phi_{GC} &= R' \sqrt{\frac{k_r}{D}} \\ R' &= r_p \text{ for a sphere} \\ h(f) &= 3f - 1 \end{aligned} \tag{4.46}$$

In this approach, not the characteristic length, but the efficiency-modulus relationship is influenced by partial wetting and it is therefore completely different from (4.33) where

the characteristic length is adjusted according to the fractional wetting.

The performance of this "modified GC model" is shown as a parity plot in Figure 4.4, and is even better than the traditional generalised modulus approach. The cylinder shell model of Valerius et al. (1996b) performs well, but is limited to $f > 0.5$. The treatment

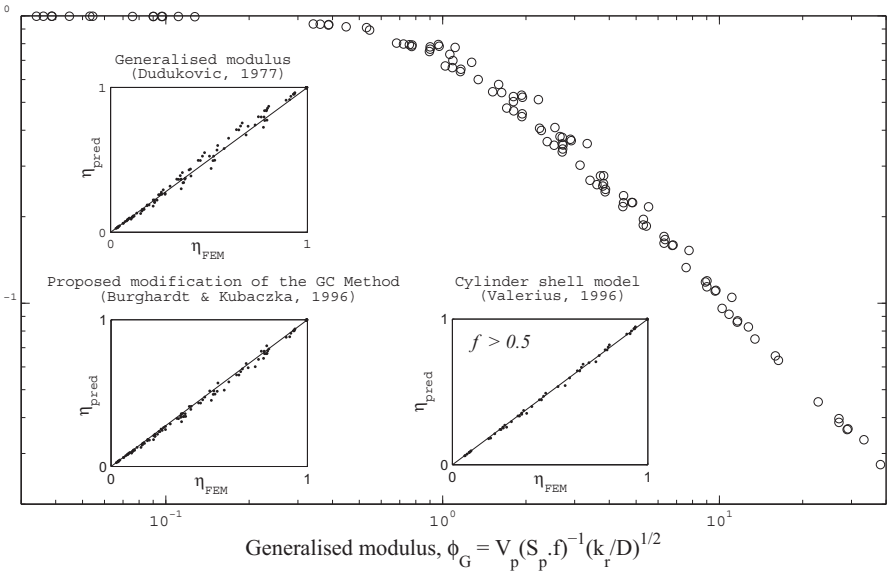

Figure 4.4: Particle efficiency versus generalised modulus for partially wetted particles and liquid-limited reaction conditions for real wetting geometries. The parity plots show the prediction performance for the discussed models for liquid-limited particle efficiency.

of external mass transfer for liquid-limited reactions is analytically correct and need not be verified.

Gas-limited reactions

The most important model for the evaluation of partially wetted particle efficiency under gas-limited conditions is the "weighting method" of Ramachandran and Smith (1979), Equation (4.37). This weighting method should be accurate if the difference between dry and wet surface concentrations is small, so that unsymmetrical boundary conditions do not have a major influence on the concentration profiles in the slab (Ramachandran and Smith, 1979). Usually, Bi_d is very high and it was therefore investigated for which values of Bi_w the weighting method would still be accurate when external mass transfer limitations on the dry part of the catalyst were negligible. Results are shown as parity plots in Figure 4.5. Liquid-solid mass transfer Biot numbers are typically larger than 10 for trickle-bed reactor applications (see Figure 2.3) as is also the case for gas-liquid mass transfer (see database reported by Iliuta et al. (1999)). It can be concluded that equation (4.37) clearly yields accurate results for realistic values of Bi_w.

The only significant source of prediction error is the fact that slab geometry is used to model other pellet geometries (spherical in this work), as can be seen from the subplot in the bottom right corner. The equivalent of Equation (4.37) for a sphere is:

$$\eta_0 = \frac{3f\left(\phi\coth\phi - 1\right)}{\phi^2\left(1 + \frac{\phi\coth\phi - 1}{Bi_w}\right)} + \frac{3(1-f)\left(\phi\coth\phi - 1\right)}{\phi^2\left(1 + \frac{\phi\coth\phi - 1}{Bi_d}\right)} \tag{4.47}$$

Though the original derivation of Equation (4.37) by Ramachandran and Smith (1979) was only valid for the slab geometry defined in that work, Goto et al. (1981) have shown that one can also use Equation (4.47), as can also be seen from the FEM results.

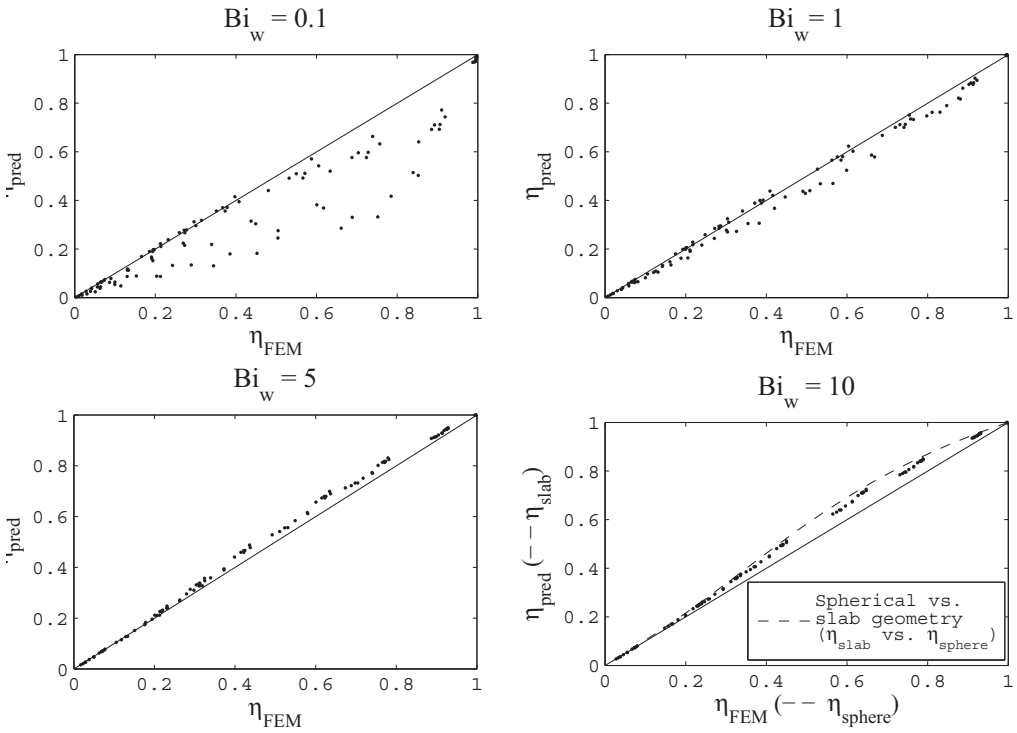

Figure 4.5: Parity plots of pellet efficiency factors as calculated with the weighting model vs. FEM results for different extents of mass transfer resistances over the wetted part of the catalyst if gas-solid mass transfer is negligible. In the last subplot, the parity between spherical and slab efficiency at the same generalised modulus is also shown.

The Bischoff modulus

For a completely wetted particle, the Bischoff modulus[7] (based on surface concentrations) for the reaction $r_A = \alpha r_B = -\alpha k_r C_A C_B$ can be derived as follows, starting at the

[7]The work in this chapter makes use of the "spherical" modulus, Equation (4.45)

definition of the Bischoff modulus:

$$\phi_T = \frac{3V_p \cdot r(C_s)}{S_p\sqrt{2D}} \left(\int_{C_{eq}}^{C_s} r(\beta) d\beta \right)^{-1/2} \tag{4.48}$$

This definition allows for the integration of a reaction rate which is decribed in terms of one reagent only. If $\gamma > 1$, $C_{A,eq} = 0$ and $C_{B,eq}$ is unknown, so that C_B should be written in terms of C_A. This can be done by using Equation (4.24), which relates the concentrations of A and B in the pellet:

$$\begin{aligned}
\phi_T &= \frac{3V_p \cdot r(C_{A,s}, C_{B,s})}{S_p\sqrt{2D_A}} \left(\int_0^{C_{A,s}} r(C_A) dC_A \right)^{-1/2} \\
&= \frac{r_p \cdot \alpha k_r C_{A,s} C_{B,s}}{\sqrt{2D_A}} \left(\int_0^1 \alpha k_r C_{A,s}^2 C_{B,s} a \left(\frac{a - 1 + \gamma'}{\gamma'} \right) da \right)^{-1/2} \\
&= \frac{r_p\sqrt{\alpha \cdot k_r C_{B,s}}}{\sqrt{2D_A}} \left(\int_0^1 \frac{a^2 - a + \gamma' a}{\gamma'} \right)^{-1/2} \\
&= \frac{\phi'_A}{\sqrt{2}} \left[\left(\frac{a^3}{3\gamma'} - \frac{a^2}{2\gamma'} + \frac{1}{2} \right) \Big|_0^1 \right]^{-1/2} \\
&= \phi'_A \left(1 - \frac{1}{3\gamma'} \right)^{-1/2}
\end{aligned} \tag{4.49}$$

when $\gamma' < 1$, $C_{B,eq} = 0$ and the above derivation should be performed in terms of C_B to obtain:

$$\phi_T = \phi'_B \left(1 - \frac{\gamma'}{3} \right)^{-1/2} \tag{4.50}$$

In this derivation a and b are dimensionless concentrations based on *surface* concentrations. Either equation (4.49) or (4.50) can be used when $\gamma' = 1$, since the equilibrium concentration of both reagents will then be equal to zero. Pellet effectiveness factors for completely wetted particles, $r_A = \alpha r_B = -\alpha k_r C_A C_B$ and negligible external mass transfer were calculated using FEM. These are shown as a function of the above derived Bischoff modulus in Figure 4.6. Clearly, the Bischoff modulus for this reaction can be used for a good approximation of pellet efficiency.

Equation (4.24), describing the relationship between a and b for complete wetting, is valid for *any* power law reaction $r_A = \alpha r_B = -k_r C_A^n C_B^m$, and one can write a general

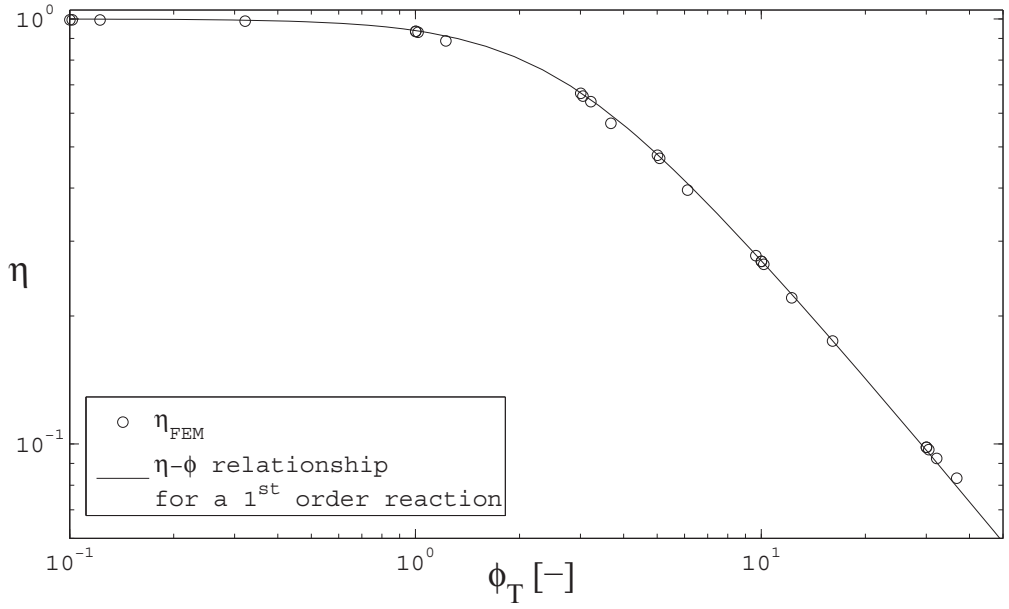

Figure 4.6: Pellet efficiency factors as a function of the Bischoff modulus for the reaction $r_A = \alpha r_B = -\alpha k_r C_A C_B$, fully wetted particles with no external mass transfer resistances. Also shown is the η-ϕ relationship for a first-order reaction in a sphere

expression for the Bischoff modulus for these types of reactions[8]:

$$\phi_T = \frac{\phi'_A}{\sqrt{2}} \left(\int_0^1 a^n \left(\frac{a-1+\gamma'}{\gamma'} \right)^m da \right)^{-1/2} \quad \gamma = \left(\frac{\phi'_A}{\phi'_B} \right)^2 > 1$$
$$\phi_T = \frac{\phi'_B}{\sqrt{2}} \left(\int_0^1 \left(\gamma' b + 1 - \gamma' \right)^n b^m db \right)^{-1/2} \quad \gamma = \left(\frac{\phi'_A}{\phi'_B} \right)^2 < 1 \tag{4.51}$$

Where:

$$\phi'_A = r_p \sqrt{\frac{\alpha k_r C_{A,s}^{n-1} C_{B,s}^m}{D_A}}; \quad \phi_B = r_p \sqrt{\frac{k_r C_{A,s}^n C_B^{m-1}}{D_B}} \tag{4.52}$$

The FEM investigation was performed for $n = 1$ and $m = 1$ only, as stated previously.

4.2.3 A unified model for $r_A = \alpha r_B = -\alpha k_r C_A C_B$

The previous section has shown that the existing models for liquid- and gas-limited reactions are satisfactory for true wetting geometries. These models are specific to either liquid- or gas-limited reactions but provide useful descriptions of the effect of partial wetting on the behaviour of the liquid and gaseous reagents, that can be summarised as follows:

- For liquid-limited reactions, the generalised modulus approach (Dudukovic, 1977)

[8]The dimensionless concentration term in the reaction expression does not play a role in the derivation of the relationship between a and b, see Appendix A

can be recommended, giving acceptable predictions while being very simple to use. According to this approach, partial wetting affects the effective geometry (diffusion path length) of the limiting reagent when a reaction is liquid-limited. For a monodispersed catalyst pellet, the Thiele modulus of a partially wetted particle can be corrected for partial wetting by adjusting the effective geometry so that $\phi_{corr} = \phi/f$. Where in the previous discussion the Thiele modulus-efficiency relationship of a slab was used for any geometry, it is also possible to use that of a sphere. Overall pellet efficiency can be evaluated by taking external mass transfer resistances into account as is shown in Equation (4.35). Mathematically, the approach to liquid-limited reactions can be written as:

$$\eta_0 = \eta\left(\phi_B''/f\right) \times \frac{C_{B,s}}{C_{B,bulk}} \tag{4.53}$$

- Partial wetting affects the average external surface concentration of the limiting reagent when the reaction is gas-limited. Correcting overall pellet efficiency with the average external surface concentration weighted according to the fractional wetting, yield good results for realistic rates of external mass transfer. It is preferable to use the model of Ramachandran and Smith (1979) in conjunction with the Thiele modulus - pellet efficiency relationship specific to the particle geometry.

$$\eta_0 = \eta\left(\phi_A'\right) \times \frac{fC_{A,s}|_w + (1-f)C_{A,s}|_d}{C_{A,bulk}} \tag{4.54}$$

Combining the above approaches with the Bischoff modulus derived for the reaction $r_A = \alpha r_B = -\alpha k_r C_A C_B$, the following unified model for this reaction is suggested to

predict the efficiency of partially wetted particles over the whole γ-range:

$$\eta_0 = \frac{3\overline{C_{A,s}}C_{B,s}}{\phi_T^2 C_A^* C_{B,bulk}}\left(\phi_T \coth \phi_T - 1\right) \tag{4.55}$$

$$\phi_T = \phi'_A\left(1 - \frac{{\phi'_B}^2}{3{\phi'_A}^2}\right)^{-1/2} \quad \phi'_A \geq \phi'_B$$

$$\text{or } \phi_T = \phi'_B\left(1 - \frac{{\phi'_A}^2}{3{\phi'_B}^2}\right)^{-1/2} \quad \phi'_A < \phi'_B \tag{4.56}$$

$$\phi'_A = r_p\sqrt{\frac{k_r C_{B,s}}{D_A}}; \quad \phi'_B = \frac{r_p}{f}\sqrt{\frac{k_r \overline{C_{A,s}}}{D_B}} \tag{4.57}$$

$$\overline{C_{A,s}} = C_A^*\left[f\left(1 + \frac{{\phi'_A}^2\left(\phi_T \coth \phi_T - 1\right)}{\phi_T^2 Bi_{A,w}}\right)^{-1}\right.$$
$$\left. + \ (1-f)\left(1 + \frac{{\phi'_A}^2\left(\phi_T \coth \phi_T - 1\right)}{\phi_T^2 Bi_{A,d}}\right)^{-1}\right] \tag{4.58}$$

$$C_{B,s} = C_{B,bulk}\left(1 + \frac{{\phi'_B}^2 f\left(\phi_T \coth \phi_T - 1\right)}{\phi_T^2 Bi_{B,w}}\right)^{-1} \tag{4.59}$$

The model treats gas and liquid reagents according to the traditional approaches: the average surface concentration of the gas and the modulus for the liquid component are affected by fractional wetting according to the models of Ramachandran and Smith (1979) and Dudukovic (1977) respectively. The liquid external surface concentration is calculated according to Equation (4.30). The major discrepancy in this model is that it uses a Bischoff modulus that was derived for fully wetted particles, but the results are good for a wide γ-range, as is shown in Figure 4.7, especially when compared to predictions of the traditional liquid-limited and gas-limited models shown in Figure 4.8. As for Equation (4.37), the unified model makes uses an overall gas-liquid-solid Biot number, assuming equal rates of gas-liquid and liquid-solid mass transfer. If this does not apply, the wetted surface concentration of A should be evaluated in a similar fashion as that shown in equation (4.38). The unified model is reported here in terms of spherical particles, but there is no reason why it cannot be applied to other shapes, since the principles of the model are not based on particle geometry.

4.3 Eggshell particles

The first, and probably most obvious, difference between monodispersed and eggshell catalyst spheres is that the latter tend to behave like a slab as the shell thickness decreases. This can best be seen from the definition of h in the GC model: $h = 0$ for a slab, and

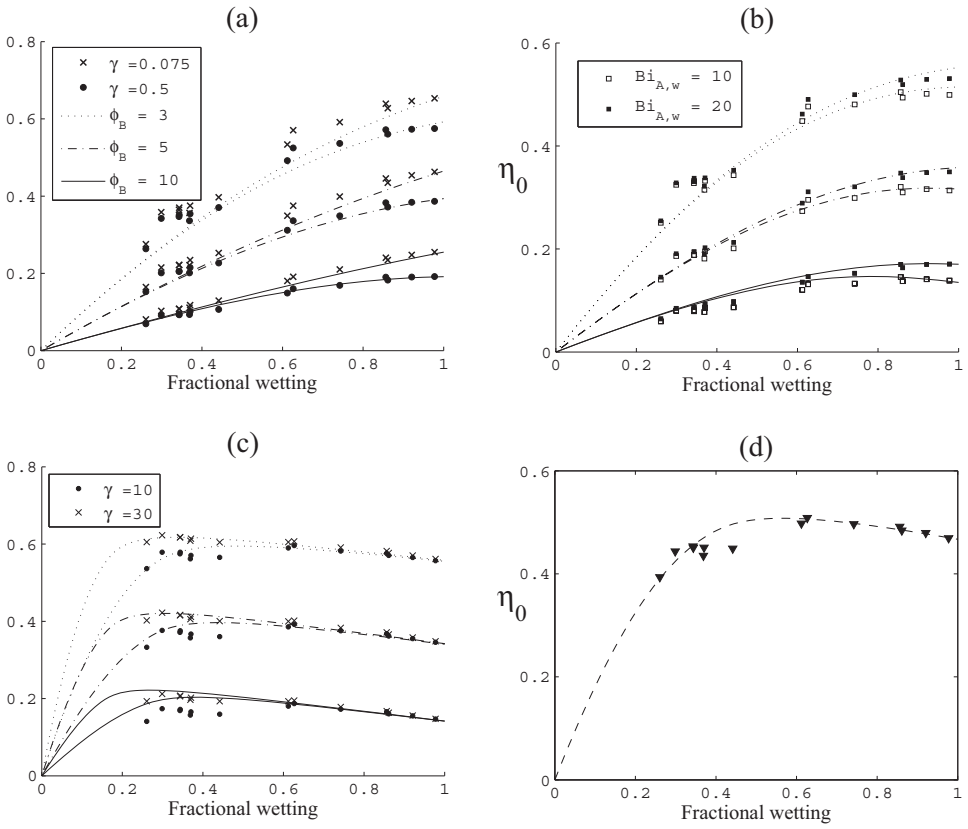

Figure 4.7: Performance of the unified model for the reaction $r_A = \alpha r_B = -\alpha k_r C_A C_B$. (a) Liquid-limited reaction, with some external mass transfer resistances for the gaseous reagent over the wetted surface ($Bi_{A,w} = 10$, $Bi_{A,d} \to \infty$, $Bi_{B,w} \to \infty$); (b) reaction that is not classified as either gas or liquid-limited with varying rates of external mass transfer for the gaseous reagent ($\gamma = 1$, $Bi_{A,d} \to \infty$, $Bi_{B,w} \to \infty$); (c) gas-limited reaction ($Bi_{A,w} = 10$, $Bi_{A,d} \to \infty$, $Bi_{B,w} \to \infty$); (d) arbitrarily chosen conditions ($\phi_A = 3$, $\gamma = 5$, $Bi_{A,w} = 5$, $Bi_{A,d} = 50$, $Bi_{B,w} = 10$). All Thiele moduli are as defined in the legend of subfigure (a).

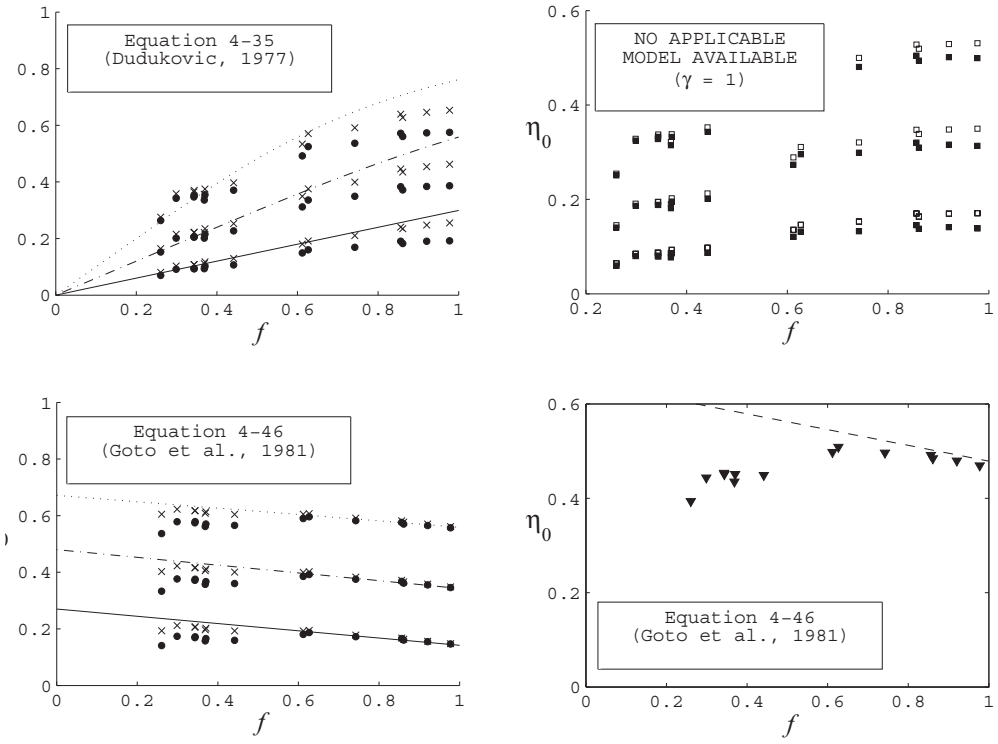

Figure 4.8: Predictions of the FEM data in Figure 4.7 by traditional models for liquid- and gas-limited reactions.

$h = 2$ for a sphere. For an eggshell sphere of inner to outer shell diameter ratio ρ:

$$\begin{aligned} h &= \frac{S_p}{V_p} R' - 1 \\ &= \frac{4\pi r_p^2}{4/3\pi r_p^3 \left(1-\rho^3\right)} \cdot r_p \left(1-\rho\right) - 1 \\ &= \frac{3\left(1-\rho\right)}{1-\rho^3} - 1 \end{aligned} \tag{4.60}$$

in the limit of $\rho \rightarrow 1$, $h \rightarrow 0$, which suggests slab geometry. Gas-limited reactions in partially wetted egshell particles clearly show "slab behaviour": for the investigated eggshell catalysts, Equation (4.37), which assumes slab geometry, works very well for $Bi_w \geq 5$ (within 5% accuracy for all simulation results). Another reason why gas-limited reactions within an eggshell catalyst can be predicted so well, is that the dry and wetted parts of the reaction zone are more segregated than in a monodispersed catalyst.

Liquid limititations are not predicted well by the traditional generalised modulus approach and incomplete wetting has a more detrimental effect than on monodispersed catalysts, as is shown in Figure 4.9. The reason why the generalised modulus approach performs so poorly for a partially wetted eggshell catalyst, is that a zone exists where diffusion without reaction takes place. The particle can therefore not be directly related

to a slab with diffusion and reaction throughout its volume. Due to symmetry, such zones will not exist in a fully wetted particle, so that the generalised modulus approach works well for eggshell catalysts with a high wetting efficiency.

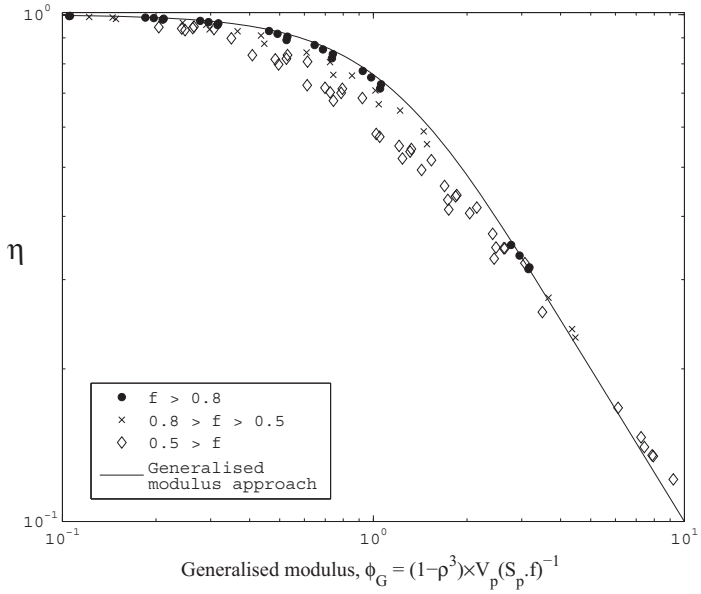

Figure 4.9: Particle efficiency versus generalised modulus for partially wetted particles and liquid-limited reaction conditions for real wetting geometries on a spherical eggshell catalyst ($\rho = 0.9$).

Similarly to the generalised modulus approach, it is difficult to define the characteristic length to use in the GC method (Equation (4.29, defined as the maximum distance for diffusion under reaction conditions). For a fully wetted particle this should be equal to $r_p\,(1-\rho)$, but for a fractionally wetted particle substantially more. To be consistent with the modified GC method proposed in section 4.2.2 (equation 4.46), the characteristic length for $\rho = 0$ should be equal to r_p, independent of the fractional wetting. It is possible to define a general expression for the characteristic length that meets these requirements:

$$R^{'} = r_p\,(1 - \rho \times g(f)) \tag{4.61}$$

The shape factor, h is then given by:

$$h = \frac{S_x}{V_R} R^{'} - 1 = \frac{3f \times (1 - \rho \times g(f))}{1 - \rho^3} - 1 \tag{4.62}$$

where $g(f)$ should be equal to 1 for $f = 1$. Also, $R^{'}$ should increase and $g(f)$ should decrease as f decreases, most likely in a non-linear function. Assuming a quadratic relationship between $g(f)$ and f, the following function was fitted onto FEM efficiency data for a liquid-limited reaction in eggshell catalysts with shell dimensions of $\rho = 0.9$

and $\rho = 0.5$:

$$g(f) = k_1\left(f^2 - 1\right) + k_2\left(f - 1\right) + 1 \tag{4.63}$$

Best-fit values for k_1 and k_2 are -2 and 4, respectively. Equations (4.61) to (4.63) simplify to Equations (4.46) for a monodispersed catalyst. The equations imply slab geometry for very thin eggshells ($h \to 0$ when $\rho \to 1$ and $f = 1$), which is also correct. The fitted parameter values for $g(f)$ suggest a limit of $R' = r_p(1 + \rho)$ when $f = 0$. Figure 4.10 shows the performance of the proposed partial wetting GC model for eggshell catalysts. Though empirical, the model performs well for $\rho = 0.9$, $\rho = 0.5$ and $\rho = 0$ (see figure 4.4 for the performance of the modified GC model when $\rho = 0$). No statement can be made about the model's performance when $\rho > 0.9$ or for shapes other than spheres[9]. External mass transfer can be accounted for in the normal fashion (Equation 4.30 or 4.32).

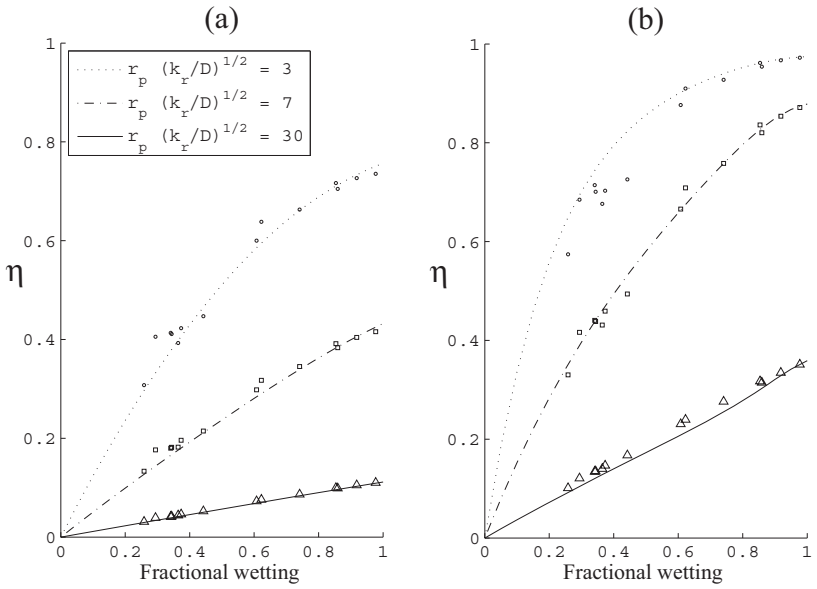

Figure 4.10: Proposed GC model for liquid-limited, partially wetted eggshell catalysts as compared with results from FEM simulations for different shell thicknesses: (a) $\rho = 0.5$ and (b) $\rho = 0.9$.

It is not possible to use the modified GC model together with the Bischoff modulus to obtain a unified model for eggshell catalysts, since the modulus-efficiency relationship varies with shape in the GC model. For this reason a generalied modulus-type description is needed for eggshell catalysts. Based on the limits of R' in the GC model for egghell particles ($R' = (1 - \rho)$ for fully wetted particles, and $r_p\,(1 + \rho)$) and the generalised modulus for a fully wetted particle, the following correction of the generalised modulus

[9]An exception is for the case where $\rho = 0$. Here, it should be clear from the work of Burghardt and Kubaczka (1996) how to adjust Equation (4.46) for shapes other than spheres. The accuracy should be more or less the same as that shown in Figure 4.4

is suggested for eggshell particles:

$$\phi_G = \underbrace{\phi\frac{(1-\rho^3)}{3f}}_{\phi_G \text{ for partially wetted eggshell sphere}} \times \underbrace{[1+\rho(1-f)]}_{\text{correction factor}} \tag{4.64}$$

This modified generalised modulus for eggshell catalysts works rather well, especially for thin shells, as is shown in Figure 4.11. Though possibly somewhat less accurate than the modified GC model, this generalised eggshell modulus is far easier to use and can also be used in the unified model. To model eggshells with both liquid and gas reagent limitations, one should make use of slab geometry so that the unified model becomes:

$$\eta_0 = \frac{\overline{C_{A,s}}C_{B,s}}{\phi_T C_A^* C_{B,bulk}}\tanh\phi_T \tag{4.65}$$

$$\begin{aligned}
\phi_T &= \phi'_A\left(1-\frac{{\phi'_B}^2}{3{\phi'_A}^2}\right)^{-1/2} \quad \phi'_A \geq \phi'_B \\
\text{or } \phi_T &= \phi'_B\left(1-\frac{{\phi'_A}^2}{3{\phi'_B}^2}\right)^{-1/2} \quad \phi'_A < \phi'_B \\
\phi'_A &= \frac{r_p(1-\rho^3)}{3}\sqrt{\frac{k_r C_{B,s}}{D_A}} \\
\phi'_B &= \frac{r_p(1-\rho^3)(1+\rho-\rho\cdot f)}{3f}\sqrt{\frac{k_r\overline{C_{A,s}}}{D_B}}
\end{aligned} \tag{4.66}$$

$$\begin{aligned}
\overline{C_{A,s}} &= C_A^*\left[f\left(1+\frac{{\phi'_A}^2\tanh\phi_T}{\phi_T Bi'_{A,w}}\right)^{-1}\right. \\
&+ \left.(1-f)\left(1+\frac{{\phi'_A}^2\tanh\phi_T}{\phi_T Bi'_{A,d}}\right)^{-1}\right]
\end{aligned} \tag{4.67}$$

$$C_{B,s} = C_{B,bulk}\left(1+\frac{{\phi'_B}^2 f\tanh\phi_T}{\phi_T Bi_{B,w}}\right)^{-1} \tag{4.68}$$

Performance of the unified model for eggshell catalysts is shown in figure 4.12.

4.4 Summary

The wetting geometries obtained from the colorimetric work in Chapter 3 were used to investigate the effects of partial wetting on intraparticle diffusion, using FEM simulation. It was shown that existing models can predict the effectiveness factor of monodispersed catalyst particles satisfactorily for true wetting geometries for both liquid- and gas-limited reactions. These models are limited to first-order reactions, with a rate dependence only on either the gas or the liquid reagent. Adopting the traditional descriptions for partial

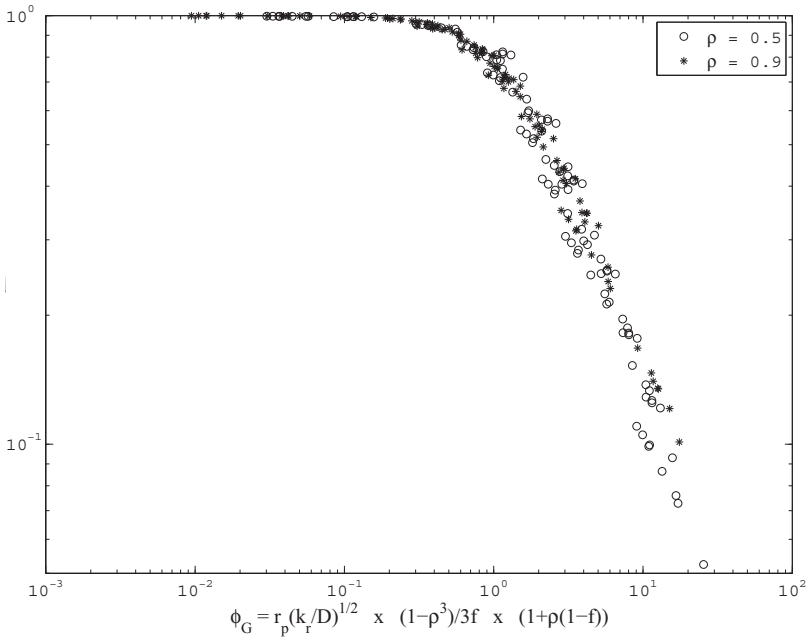

Figure 4.11: Pellet efficiency for partially wetted spherical eggshell catalysts as a function of the modified eggshell modulus (Equation 4.64)

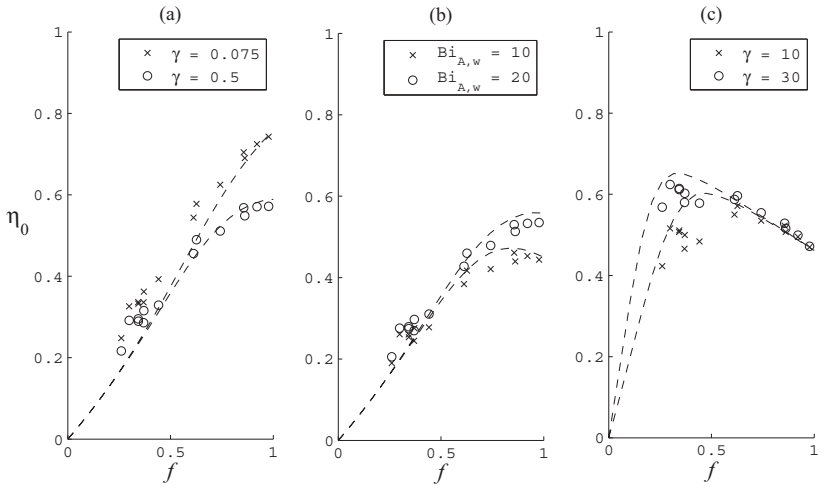

Figure 4.12: Overall efficiency factor for the reaction $-r_A = k_r C_A C_B$ in an eggshell catalyst where $\rho = 0.9$. (a) Liquid-limited reaction with some external mass transfer resistances for the gaseous reagent over the wetted surface ($Bi_{A,w} = 10$, $Bi_{A,d} \rightarrow \infty$, $Bi_{B,w} \rightarrow \infty$); (b)reaction that is not classified as either gas- or liquid-limited with varying rates of external mass transfer for the gaseous reagent ($\gamma = 1$, $Bi_{A,d} \rightarrow \infty$, $Bi_{B,w} \rightarrow \infty$); (c) gas-limited reaction ($Bi_{A,w} = 10$, $Bi_{A,d} \rightarrow \infty$, $Bi_{B,w} \rightarrow \infty$). For all data, $\phi_i = 10$ where i refers to the limiting reagent.

wetting effects on liquid- and gas-limited reactions, a unified model was developed for the reaction $r_A = -\alpha r_B = \alpha k_r C_A C_B$. This unified model can be used over the whole γ-range, so that a reaction need not be classified as either liquid- or gas-limited.

Eggshell catalysts have not previously been studied for trickle-bed reactor purposes, though these are quite common for hydrogenation purposes. Based on FEM results, models are suggested to estimate the effect of partial wetting on eggshell particles for any value of γ. It was shown that, in term of liquid-limitations, eggshell particles are more sensitive to partial wetting than monodispersed particles.

Nomenclature

A_1, B_1	quantities defined in Equation (4-23), dimensionless
a	dimensionless concentration of reagent A
a_p	ratio of catalyst surface area to catalyst volume in a reactor, m^{-1}
a_{GL}	ratio of gas-liquid surface area to catalyst volume in a reactor, m^{-1}
b	dimensionless concentration of reagent B
Bi	Biot number for a sphere, dimensionless
Bi'	Biot number based on slab geometry, $Bi' = \frac{V_R k_c}{S_p D}$
Bi''	Biot number based on slab geometry and the external area available for mass transfer, $Bi' = \frac{V_R k_c}{S_x D}$
c	dimensionless concentration, $c = \frac{C}{C_{bulk}}$
$C*$	saturation concentration, $^{\mathrm{mol}}/_{\mathrm{m}^3}$
C_i	concentration of reagent i, $^{\mathrm{mol}}/_{\mathrm{m}^3}$
C_{eq}	concentration for which reaction rate is zero, $^{\mathrm{mol}}/_{\mathrm{m}^3}$
C_L	concentration in centre of slab, $^{\mathrm{mol}}/_{\mathrm{m}^3}$
D_i	effective diffusivity of reagent i, $^{\mathrm{m}^2}/_{\mathrm{s}}$
f	fractional wetting, dimensionless
$g(f)$	fitted function to describe the η - f relationship for an eggshell particle based on the GC model
h	shape factor for the GC model
$I_x(y)$	modified Bessel function of the first kind, order x, evaluated at y
$K_x(y)$	modified Bessel function of the second kind, order x, evaluated at y
k_r	reaction rate constant, based on active catalyst volume, units dependent on rate expression
k_R	first-order reaction rate constant, based on catalyst volume in reactor, $^{1}/_{\mathrm{s}}$
k_c	mass transfer coefficient for relevant mass transfer step, $^{\mathrm{m}}/_{\mathrm{s}}$
k_{GL}	gas-liquid mass transfer coefficient, $^{\mathrm{m}}/_{\mathrm{s}}$
k_{LS}	liquid-solid mass transfer coefficient, $^{\mathrm{m}}/_{\mathrm{s}}$
L	slab thickness, or V_R/S_x
$\overline{n}$	unit vector normal to external surface, dimensionless
r_C	radius of semi-infinite cylinder
r_p	radius of spherical particle, m
r_i	rate of production of component i, $^{\mathrm{mol}}/_{\mathrm{s}}$
R'	characteristic diffusion length for the GC model, m
R_i	residual for the estimation of dimensionless concentration i, dimensionless
s	FEM surface triangle area, dimensionless
S_p	external surface area of catalyst particle, m^2
S_x	external surface area of catalyst particle over which mass transfer can take place, m^2
v	FEM element volume, dimensionless
V_c	volume of catalyst in a reactor, m^3
V_p	volume of catalyst particle, m^3
V_R	volume of catalyst particle in which reaction can take place. The same as V_P for a monodispersed particle, but not for an eggshell particle
w	arbitrary weighting function used in the derivation of FEM equations
x	dimensionless position in a slab
$y(C)$	concentration-dependent term in the kinetic description of reaction rate, units dependent on kinetic expression

Greek letters

α	stoichiometric coefficient, dimensionless
ϕ''	Thiele modulus relevant to specifiec geometry, dimensionless
ϕ_C	Thiele modulus for a cylinder, dimensionless
ϕ_G	generalised modulus, $L\sqrt{k_r/D}$ for a first-order reaction, dimensionless
ϕ_{GC}	modulus for the GC model, dimensionless
ϕ_i	Thiele modulus of component i for a sphere. For a first-order reaction, $\phi = r_p\sqrt{\frac{k_r}{D}}$. Note that this definition is not adjusted for an eggshell catalyst.
ϕ_i'	same as ϕ_i, but based on surface concentrations for higher-order reactions, dimensionless
ϕ_T''	Bischoff modulus for a slab
ϕ_T	Bischoff modulus for a (partially wetted) sphere
γ	$(\alpha C_{B,bulk} D_B) \,/\, (C_A^* D_A)$, dimensionless
η	pellet efficiency factor, dimensionless
η_0	overall efficiency factor, dimensionless
λ	dimensionless radial position in a spherical particle
λ'	same as λ, but based on surface concentrations, dimensionless
ρ	ratio of shell inner to outer diameter, dimensionless

Subscripts

A	refers to reagent in the gas
B	refers to non-volatile reagent
$bulk$	refers to bulk liquid
d	refers to dry external area
w	refers to wetted external area
s	refers to surface